

Rings in above-threshold ionization: A quasiclassical analysis

M. Lewenstein,^{1,2} K. C. Kulander,^{1,3} K. J. Schafer,³ and P. H. Bucksbaum⁴

¹*Joint Institute for Laboratory Astrophysics, University of Colorado, Boulder, Colorado 80309-0440*

²*Centrum Fizyki Teoretycznej, Polska Akademia Nauk, Warszawa, 02-668 Poland*

³*Theoretical Atomic and Molecular Physics (TAMP), Physics Department, Lawrence Livermore National Laboratory, Livermore, California 94550*

⁴*Physics Department and Center for Ultrafast Optical Science, University of Michigan, Ann Arbor, Michigan 48109-1120*

(Received 9 August 1994)

A generalized strong-field approximation is formulated to describe atoms interacting with intense laser fields. We apply it to determine angular distributions of electrons in above-threshold ionization (ATI). The theory treats the effects of an electron rescattering from its parent ion core in a systematic perturbation series. Probability amplitudes for ionization are interpreted in terms of quasiclassical electron trajectories. We demonstrate that contributions from the direct tunneling processes in the absence of rescattering are not sufficient to describe the observed ATI spectra. We show that the high-energy portion of the spectrum, including recently discovered rings (i.e., complex features in the angular distributions of outgoing electrons) are due to rescattering processes. We compare our quasiclassical results with exact numerical solutions.

PACS number(s): 32.80.Rm, 42.65.Ky

I. INTRODUCTION

In recent years, there has been considerable progress in understanding strong-field laser-atom interactions due to the development of the two-step, strong-field ionization model [1]. The model, which combines quantum and classical aspects of the laser-atom interactions, proved to be very useful in explaining [2,3] high harmonic generation (HG) [4,5], and especially the location of the cut-off [6] in the HG spectra. According to this model, the electron first tunnels [7,8] from the ground state of the atom through the barrier formed by the Coulomb potential and the laser field, creating an electron wave packet of continuum states each time the field passes through its maximum amplitude. The subsequent motion of the excited electron can be treated classically, and primarily consists of the free charge oscillating along the direction of polarization of and in phase with the laser field. The electron might come back into the vicinity of the nucleus and recombine back into the ground state, emitting a photon. If it returns with a kinetic energy E_{kin} , the photon energy will be $E_{\text{kin}} + I_p$, where I_p is ionization potential. This has been shown [2,3] to be the source of recently observed [4,5] very high-order harmonic emission. Additionally, when the electron rescatters it might also change its direction and drift energy in the field, producing a photoelectron energy distributions which can include high-energy electrons, possibly with structured angular distributions. The focus of this paper is to describe calculations of photoelectron spectra in this regime and to discuss the dynamics of the emission process.

Recently, L'Huillier *et al.* [9] and Lewenstein *et al.* [10] formulated a fully quantum theory valid in the tunneling limit ($U_p \geq I_p > \omega$), where $U_p = E^2/4\omega^2$ is the ponderomotive potential, i.e., the mean kinetic energy acquired by the electron in the laser field of amplitude E and fre-

quency ω . The theory, which is a version of Keldysh-Faisal-Reiss (KFR) approximation [7], not only recovers the semiclassical picture of the two-step model, but includes the effects of quantum tunneling, quantum diffusion, and interference. Particularly fruitful was the quasiclassical analysis of this theory in terms of the saddle point method, when one looked at the propagation of the electronic wave packet in the time interval between the transitions into the continuum and back to the ground state. It turns out that within this analysis one can identify trajectories of the electron in phase space that contribute most strongly to particular transition amplitudes, just as it is done within the path integral formulation of quantum mechanics [11]. We call those trajectories quasiclassical, since although they follow classical Newtonian dynamics, the dynamics must take place in the complex domain to account for tunneling [8].

Recently, two laboratories [12–14] reported features in above threshold ionization (ATI) of noble gases excited by linearly polarized fields. The angular distributions of electrons in the ATI spectrum are typically aligned along the polarization axis. They found that this is not true for few high-energy peaks, which exhibit highly structured and much broader angular distributions, including rings. These side lobes on the angular distributions appear as rings because of the cylindrical symmetry of the system Hamiltonian about the polarization axis. It was observed that the rings are present only for electronic energies in the range near $(8-10)U_p$. It has been proposed [15] that rings are attributable to electron rescattering by the parent ion core. Rings have been observed in numerical simulations of Schafer and Kulander [16], and a “naked-eye” analysis of the time-dependent dynamics of the electronic wave packet indicates that they are indeed at least to some extent caused by rescattering [15]. Although in experiments and in numerical simulations the appearance and strength of the rings depend on the

noble gas used, the proposed interpretation in terms of a rescattering process and scaling with U_p seems to be universally valid. Note that both experiments and theory have dealt with the case $U_p < I_p$, which is, strictly speaking, not in the tunneling regime. Numerical simulations suggest, however, that for $U_p > I_p$ the appearance of these off-axis structures could be even more pronounced.

The numerical solutions of the time-dependent Schrödinger equation (TDSE) describing an atom interacting with the intense laser field, in principle, provide a full quantum description of the ATI spectra. Unfortunately, these calculations require a large amount of computing time and are impractical for spectra containing very high-energy electrons, so that results have been obtained only for a restricted regime of parameters. Therefore, it seems reasonable to seek a simpler theory which would (a) allow the generation of results for a wider range of parameters; (b) allow for intuitive physical interpretation.

According to KFR theory, sometimes termed the *strong-field approximation* (SFA), ATI spectra result from the direct tunneling processes only. Strong-field approximation neglects the effects of electron returns to the nucleus and rescattering. In the tunneling regime, electrons are promoted to the continuum with relatively small drift energies so that the oscillating field has a high probability, approximately 1/2, of driving the electron back across the plane of its parent ion, possibly changing its energy and direction. Therefore, these collisions play an important role in the final state distributions. Thus, in this paper, we present a *generalized strong-field approximation* (GSFA), which treats the effects of electron rescattering in a systematic perturbation expansion. Generalized strong-field approximation is formulated along the lines of Ref. [17] which describes, to our knowledge, the first systematic attempt to refine SFA in that respect. Also, to get a better physical understanding we perform quasiclassical analysis of the electron ionization amplitudes. We show that the zeroth-order solutions in our perturbation series describe direct tunneling processes and are dominated by two families of relevant complex trajectories. Such trajectories in the limit $I_p \rightarrow 0$ describe an electron leaving the nucleus at some time t with approximately zero velocity. The first-order solutions that account for electron rescattering are dominated by several families of relevant trajectories. These trajectories correspond in the limit $I_p \rightarrow 0$ to electrons leaving the nucleus at some time t' with near zero velocity, returning to the nucleus at later time t and "rescattering." Rescattering consists mostly in the instantaneous change of electronic *canonical momenta* without the change of its *kinetic energy* at time t . Nevertheless, since these processes occur in the presence of the laser field, they lead to redistribution of the final *kinetic momenta* of electrons as the field is turned off, or as electrons leave the laser focus.

We apply our theory to a model atom with short range potential. We show that, generally, direct tunneling processes do not describe ATI spectra correctly in the regime of parameters employed in the experiments mentioned above. Direct tunneling spectra fall off too quickly at

high energy. When rescattering is included the energy distributions fall off more slowly and well pronounced rings appear in the angular distributions for electrons with higher energies.

The plan of the paper is as follows. In Sec. II, we present the GSFA in detail, formulated as a systematic perturbative expansion in terms of part of the interaction Hamiltonian. We derive here explicit formulas for the probability amplitudes of the electron in the continuum after the turnoff of the laser pulse. In Sec. III, we define the quasiclassical analysis of the amplitudes corresponding to direct tunneling and rescattering. In Sec. IV, we introduce a model atom with short range potential. In Sec. V, we describe calculated ATI spectra for this model atom, and discuss results in various regimes of the laser parameters. In particular, we compare our results with the exact solutions of TDSE. Section V contains also our conclusions regarding this phenomenon.

II. GENERALIZED STRONG-FIELD APPROXIMATION

In this section, we discuss a generalized strong-field approximation, which is an approximate method for solving the time-dependent Schrödinger equation for an atom driven by the intense laser field. We consider the atom in a single-electron approximation under the influence of the laser field $E \sin(t)$ of linear polarization in the z direction (we use atomic units, but express all energies in terms of the photon energy). In the length gauge, the Schrödinger equation takes the form

$$i|\Psi(\mathbf{x}, t)\rangle = \left[-\frac{1}{2}\nabla^2 + V(\mathbf{x}) - E \cos(t)z \right] |\Psi(\mathbf{x}, t)\rangle. \quad (1)$$

Initially, the system is in the ground state, denoted as $|0\rangle$, which, in general, has some spherical symmetry.

We consider the case when $I_p > 1$ and when U_p is comparable or larger than I_p , so that $I_p/2U_p \leq 1$. We start our discussion by treating the case when ionization is weak, so U_p should be large, but still below the saturation level, U_{sat} , when all atoms ionize during the interaction time. In this regime of parameters, the strong-field approximation [7,8] becomes valid [18]. The intensities are large enough (10^{12} – 10^{15} W/cm²) so that intermediate resonances, including dynamically induced ones (see, for instance, [19]), play no role. The electron leaves the atoms typically when the field reaches its peak value. The effects of the force due to the potential, $-\nabla V(\mathbf{x})$, are then negligible. The electron undergoes transitions to continuum states, which we label by the kinetic momentum of the outgoing electron $|\mathbf{v}\rangle$. As it is accelerated in the field, it quickly acquires a high velocity, so that the role of $V(\mathbf{x})$ is even less pronounced.

The above considerations suggest that the following assumptions should be valid in the regime of parameters that we consider.

(a) The contribution to the evolution of the system of all bound states except the ground state $|0\rangle$ can be neglected.

(b) The depletion of the ground state can be neglected ($U_p < U_{\text{sat}}$).

(c) In the continuum, the electron can be treated as a free particle moving in the electric field with no effect of $V(\mathbf{x})$.

The detailed discussion of the validity of these assumptions, and, in particular, the most crucial assumption (c), can be found in Refs. [7,10]. There are several theoretical approaches that incorporate assumption (c) in solving Eq. (1). Ammosov *et al.* study the “classical” dynamics of the electron in the complex domain in order to describe tunneling ionization. Keldysh used a version of the \hat{S} -matrix theory with final states described by Volkov wave functions ([7], see, also, [20]). An alternative approach based on the time-reversed scattering-matrix theory has been proposed by Reiss [21]. We prefer to follow Ref. [17], since this approach is more closely related to standard methods of quantum optics and atomic physics, in the sense that it either neglects or treats as a perturbation part of the interaction Hamiltonian.

If we neglect the contribution from all other bound states except the ground state $|0\rangle$ [22], the wave function may be written in the form

$$|\Psi(t)\rangle = e^{iI_p t} \left(a(t)|0\rangle + \int d^3\mathbf{v} b(\mathbf{v}, t)|\mathbf{v}\rangle \right), \quad (2)$$

where $a(t) \simeq 1$ is the ground state amplitude, and $b(\mathbf{v}, t)$ are the amplitudes of the corresponding continuum states. We have factored out, here, free oscillations of the ground state amplitude with the bare frequency I_p . The states $|\mathbf{v}\rangle$ are the eigenstates of the free Hamiltonian corresponding to outgoing electrons with velocity \mathbf{v} ,

$$\left[-\frac{1}{2}\nabla^2 + V(\mathbf{x}) \right] |\mathbf{v}\rangle = \frac{v^2}{2} |\mathbf{v}\rangle. \quad (3)$$

Note that since we use an expansion in terms of the eigenstates of the free Hamiltonian, we can, in principle, account for the Coulombic correction to the asymptotic phase shift of the states $|\mathbf{v}\rangle$ when $V(\mathbf{x})$ is a long range potential.

To express the time evolution of the electronic state in the space spanned by $|0\rangle$ and the $|\mathbf{v}\rangle$'s, we need to know the matrix elements,

$$\langle 0|\mathbf{x}|\mathbf{v}\rangle = \mathbf{d}(\mathbf{v}) \quad (4)$$

and

$$\langle \mathbf{v}|\mathbf{x}|\mathbf{v}'\rangle = \mathbf{G}(\mathbf{v}, \mathbf{v}'). \quad (5)$$

A continuum-continuum (CC) matrix element can be expressed generally (for both short range and long range potentials) in terms of its most singular part plus the rest,

$$\mathbf{G}(\mathbf{v}, \mathbf{v}') = i\nabla_{\mathbf{v}}\delta(\mathbf{v} - \mathbf{v}') + \mathbf{g}(\mathbf{v}, \mathbf{v}'). \quad (6)$$

The first term in Eq. (6) describes the motion of a free electron in the laser field and the second term includes electron rescattering processes. On the energy shell [$v^2/2 = (v')^2/2$], the second term is related to the elas-

tic scattering amplitude for the potential $V(\mathbf{x})$. If during rescattering the electron absorbs at least one photon, $|v^2/2 - (v')^2/2| \geq 1$. Far from the energy shell, $g(\mathbf{v}, \mathbf{v}')$ should depend on momentum transfer only $\mathbf{v} - \mathbf{v}'$.

The projected Hamiltonian can be divided into two parts:

$$H = H_0 + H_1, \quad (7)$$

where

$$\begin{aligned} H_0 = & -I_p|0\rangle\langle 0| + \int d^3\mathbf{v} \frac{\mathbf{v}^2}{2} |\mathbf{v}\rangle\langle \mathbf{v}| \\ & - E \sin(t) \int d^3\mathbf{v} [d_z(\mathbf{v})|0\rangle\langle \mathbf{v}| + \text{H.c.}] \\ & - iE \sin(t) \int d^3\mathbf{v} \int d^3\mathbf{v}' |\mathbf{v}\rangle \nabla_{v_z} \delta(\mathbf{v} - \mathbf{v}') \langle \mathbf{v}'|, \end{aligned} \quad (8)$$

while

$$H_1 = -E \sin(t) \int d^3\mathbf{v} \int d^3\mathbf{v}' |\mathbf{v}\rangle g_z(\mathbf{v}, \mathbf{v}') \langle \mathbf{v}'|. \quad (9)$$

Note that H_0 includes dominant effects of the motion of the electron in the laser field, whereas H_1 accounts for the rescattering.

The generalized strong-field approximation may now be formulated to be a systematic perturbation expansion with respect to H_1 . The full Schrödinger equation for the amplitude $b(\mathbf{v}, t)$ reads

$$\begin{aligned} \dot{b}(\mathbf{v}, t) = & -i \left(\frac{\mathbf{v}^2}{2} + I_p \right) b(\mathbf{v}, t) \\ & - E \sin(t) \frac{\partial b(\mathbf{v}, t)}{\partial v_z} + iE \sin(t) d_z^*(\mathbf{v}) \\ & + iE \sin(t) \int d^3\mathbf{v}' g_z(\mathbf{v}, \mathbf{v}') b(\mathbf{v}', t). \end{aligned} \quad (10)$$

In writing Eq. (10) we have neglected the depletion of the ground state, by implicitly setting $a(t) = 1$ on the right-hand side. The evolution of the atomic state thus depends only on the form of $\mathbf{d}(\mathbf{v})$ and $\mathbf{g}(\mathbf{v}, \mathbf{v}')$.

The zeroth-order SFA corresponds to the exact solution of the Schrödinger equation for H_0 only, and it takes the form

$$\begin{aligned} b_0(\mathbf{v}, t) = & i \int_0^t dt' E \sin(t') d_z(\mathbf{v} + \mathbf{A}(t) - \mathbf{A}(t')) \\ & \times e^{-i \int_{t'}^t dt'' [(v + \mathbf{A}(t) - \mathbf{A}(t''))^2 / 2 + I_p]}, \end{aligned} \quad (11)$$

where $\mathbf{A}(t) = (E \cos(t), 0, 0)$ is the vector potential of the laser field divided by the velocity of light c .

Inserting this zeroth-order solution on the right-hand side of Eq. (10), we obtain a first-order correction to the SFA with respect to the rescattering term,

$$\begin{aligned} b_1(\mathbf{v}, t) = & - \int_0^t dt' \int_0^{t'} dt'' \int d^3\mathbf{v}' E \sin(t') \\ & \times g_z(\mathbf{v} + \mathbf{A}(t) - \mathbf{A}(t'), \mathbf{v}' - \mathbf{A}(t')) \\ & \times e^{-i \int_{t'}^t dt'' [(v + \mathbf{A}(t) - \mathbf{A}(t''))^2 / 2 + I_p]} E \sin(t'') \\ & \times d_z(\mathbf{v} - \mathbf{A}(t'')) e^{-i \int_{t''}^{t'} dt''' [(v' - \mathbf{A}(t'''))^2 / 2 + I_p]}. \end{aligned} \quad (12)$$

Assuming that the field was turned on at $t = 0$ and off at $t = t_F$ adiabatically, we may set $\mathbf{A}(0) = \mathbf{0}$. Then for $t = t_F \rightarrow \infty$, \mathbf{A} becomes equal to $\int_0^{t_F} E(t') dt'$, and is of the order of $2\sqrt{U_p}/\tau_D$, where τ_D is the duration of the laser pulse. It is quite safe, therefore, to set $\mathbf{A}(t \rightarrow \infty) = \mathbf{0}$, also. Thus, in the limit $t \rightarrow \infty$, we obtain

$$b_0(\mathbf{v}) = i \int_0^{t_F} dt' E \sin(t') d_z(\mathbf{v} - \mathbf{A}(t')) \times e^{-i \int_0^{t_F} dt'' [(v - \mathbf{A}(t''))^2/2 + I_p]}. \quad (13)$$

The interpretation of this result is straightforward. This is the total probability amplitude that the electron, excited into the continuum at time t' , had the appropriate velocity $\mathbf{v} - \mathbf{A}(t')$. The excitation amplitudes are proportional to the first two factors in the integrand of Eq. (13). They then propagate until time t_F , acquiring a phase factor $\exp(-iS(\mathbf{v}, t_F, t'))$, where $S(\mathbf{v}, t_F, t')$ is the quasiclassical action,

$$S(\mathbf{v}, t, t') = \int_{t'}^t dt'' \left(\frac{(\mathbf{v} - \mathbf{A}(t''))^2}{2} + I_p \right). \quad (14)$$

The effects of the atomic potential are assumed to be negligible during the propagation time between t' and t , so that $S(\mathbf{v}, t, t')$ actually describes the motion of an electron freely moving in the laser field with a constant canonical momentum \mathbf{v} . Note, however, that $S(\mathbf{v}, t, t')$ does incorporate the dominant effect of the binding potential through its dependence on I_p .

Similarly, for $t_F \rightarrow \infty$, the first-order term becomes

$$b_1(\mathbf{v}) = - \int_0^{t_F} dt' \int_0^{t'} dt'' \int d^3\mathbf{v}' E \sin(t') \times g_z(\mathbf{v} - \mathbf{A}(t'), \mathbf{v}' - \mathbf{A}(t')) e^{-iS(\mathbf{v}, t_F, t')} \times E \sin(t'') d_z(\mathbf{v}' - \mathbf{A}(t'')) e^{-iS(\mathbf{v}', t', t'')}. \quad (15)$$

The above expression also has a simple physical meaning. The electron makes the transitions to the continuum at t'' with the amplitude $E \sin(t'') d_z(\mathbf{v}' - \mathbf{A}(t''))$. The velocity of the electron is then $\mathbf{v}' - \mathbf{A}(t'')$. It propagates until t' when it rescatters, then propagates until t_F . The propagation in both cases consists of the accumulation of phase factors of the form i times the corresponding quasiclassical actions.

The zeroth- and the first-order solutions can be expanded in terms of ordinary or generalized Bessel functions. For instance, let

$$E \sin(t') d_z(\mathbf{v}' - \mathbf{A}(t')) = \sum_M d_M(\mathbf{v}') e^{iM t'}. \quad (16)$$

Then, up to the irrelevant phase factor,

$$b_0(\mathbf{v}) = \sum_{N \geq v^2/2 + I_p + U_p} b_{N,0}(\mathbf{v}), \quad (17)$$

with

$$b_{N,0}(\mathbf{v}) = 2\pi i \sum_{M=-\infty}^{\infty} \delta(v^2/2 + I_p + U_p - N) \times J_M(2\sqrt{U_p} v \cos(\theta), -u_p/2) d_{M-N}(\mathbf{v}), \quad (18)$$

where $J_M(\cdot)$ denotes a generalized Bessel function. This is an analog of Reiss' formula (43) in Ref. [7]. It is different, however, since we have used the length gauge, i.e., accounted for the full velocity dependence of the transition matrix element $\mathbf{d}(\mathbf{v})$.

Similarly, the first-order correction can be written in the form

$$b_1(\mathbf{v}) = \sum_{N \geq v^2/2 + I_p + U_p} b_{1,N}(\mathbf{v}), \quad (19)$$

with

$$b_{1,N}(\mathbf{v}) = (2\pi)^2 \int d^3\mathbf{v}' \sum_{M,K=-\infty}^{\infty} M J_M(2\sqrt{U_p} [\cos(\theta) - \cos(\theta')]) \delta(v^2/2 - (v')^2/2 - K) g(\mathbf{v} - \mathbf{v}') \times \delta(v^2/2 + I_p + U_p - N + K) J_M(2\sqrt{U_p} v \cos(\theta), -u_p/2) d_{M-N+K}(\mathbf{v}), \quad (20)$$

where $J_M(\cdot)$ denotes an ordinary Bessel function. The above expression refers to the situation in which $\mathbf{g}(\mathbf{v}, \mathbf{v}')$ is a function of $\mathbf{v} - \mathbf{v}'$ only. It also has a very nice physical interpretation. Namely, it is a convolution of the two transition amplitudes: the direct tunneling amplitude to the state of intermediate velocity $(v')^2/2 = N - K - I_p - U_p$, followed by a rescattering process involving the absorption of K (or emission of $-|K|$) photons to the state with velocity, \mathbf{v} , where $v^2/2 = N - I_p - U_p$. The rescattering process takes place in the presence of

the laser field. The corresponding amplitude is not only proportional to the CC matrix element, but also contains factors that describe photon absorption and emission processes. The well known Kroll-Watson formula [23-25] for electron scattering in laser fields, which has been investigated in experiments by Weingartshofer [26], is analogous to this expression for the rescattering amplitude. Although expressions (18) and (20) have many appealing properties, we shall not refer to them in the following. Instead we shall use expressions (13) and (15), evaluating

them using a saddle point and numerical approach. More generally, i.e., when $\mathbf{g}(\mathbf{v}, \mathbf{v}')$ depends explicitly on both arguments, the t' dependence of $\mathbf{g}(\mathbf{v} - \mathbf{A}(t'), \mathbf{v}' - \mathbf{A}(t'))$ cannot be eliminated. In such a case the formula (20) has a similar, but much more complex form.

III. QUASICLASSICAL ANALYSIS OF THE DIRECT TUNNELING AND RESCATTERING PROCESSES

To analyze Eqs. (13) and (15) in a quasiclassical sense, we perform the integrals in those expressions using a saddle point method. This method [9,10] is expected to be accurate when both U_p and I_p , as well as the involved velocities \mathbf{v} and \mathbf{v}' are large. Since quasiclassical actions are proportional to I_p , U_p , v^2 etc., the factors $\exp(-iS_{cl})$ are rapidly oscillating, and one should thus seek stationary points of the quasiclassical actions. Such a procedure is legitimate provided d_z and g_z are slowly varying and, in particular, nonsingular at the saddle points of the actions. Unfortunately, the latter assumption is not true, in general (see discussion in [10]), and the correct saddle point evaluation must take this fact into account. Nevertheless, the leading contribution at the saddle point is determined by requiring stationarity of the quasiclassical action [27], which captures the essential underlying physics. Therefore, in the following, we analyze Eqs. (13) and (15) in terms of the stationary points of the quasiclassical action only.

The zeroth-order term describing direct tunneling then becomes

$$b_0(\mathbf{v}, t \rightarrow \infty) = i \sum_{\text{SP}} \left(\frac{2\pi}{\det \mathcal{A}_2} \right)^{1/2} E \sin(t'_{\text{SP}}) \times d_z(\mathbf{v} - \mathbf{A}(t'_{\text{SP}})) e^{-iS_{cl}(t_F, t'_{\text{SP}})}, \quad (21)$$

where the sum is over the saddle points t'_{SP} , t_F is a final time accounting for an irrelevant phase and $\det \mathcal{A}_2$ is a determinant of the second derivative matrix, which in this case is equal to $-i(\mathbf{v} - \mathbf{A}(t'_{\text{SP}})) \cdot \mathbf{E}(t'_{\text{SP}})$.

The saddle points are derived from the condition

$$\frac{(\mathbf{v} - \mathbf{A}(t'_{\text{SP}}))^2}{2} + I_p = 0. \quad (22)$$

Note that if $I_p = 0$, the saddle points correspond simply to electron trajectories that leave the nucleus with zero kinetic momentum. In general, for $I_p \neq 0$, the trajectories are complex and there are families of pairwise complex conjugated solutions to Eq. (22). Denoting

$$t = \arccos \left(\frac{1}{\sqrt{4U_p}} \left[v \cos \theta + i \sqrt{v^2 \sin^2 \theta + 2I_p} \right] \right), \quad (23)$$

the families are $t + 2\pi k$, $-t + 2\pi k$, $t^* + 2\pi k$, and $-t^* + 2\pi k$, where k is an integer. As we see each family consists of sequence of solutions shifted by 2π . Only two of these families contribute to Eq. (21), since the action $S_{cl}(t_F, t'_{\text{SP}})$

must attain a negative imaginary part to describe appropriately the exponential decay of the ionization amplitudes.

It is interesting that even for $I_p = 0$, and $\theta = 0$, Eq. (23) has no real solutions for $v > \sqrt{4U_p}$, indicating that in this limit there is a cutoff of the ATI spectrum allowing no electron of kinetic energy larger than $2U_p$.

Denoting by t_{SP}^1 , and t_{SP}^2 the two ‘‘fundamental’’ solutions of Eq. (23) that fulfill $0 \leq \text{Im}(t'_{\text{SP}}) < 2\pi$, the sum in Eq. (21) reduces to the form of Eq. (18),

$$b_0(\mathbf{v}) = i \sum_{k=1}^2 \sum_N \left(\frac{2\pi}{\det \mathcal{A}_2} \right)^{1/2} E \sin(t_{\text{SP}}^k) d_z(\mathbf{v} - \mathbf{A}(t_{\text{SP}}^k)) \times e^{-iS_{cl}(t_F, t_{\text{SP}}^k)} \delta(v^2/2 - N - I_p - U_p). \quad (24)$$

Note that since there are two contributions to each ATI peak, the probability amplitude from direct tunneling generally displays interference effects. We stress that this is a generic feature of the dynamics which also occurs when we consider the rescattering events.

Several authors [28] have suggested that the quantum interference in direct tunneling could cause rings in angular distributions. As we see below, although interference effects are indeed present in the direct tunneling amplitudes, they cannot be associated with the rings observed in the experiments and in the exact numerical solutions.

A similar stationary phase analysis can be done for the first-order solution (15). In this case, the result is

$$b_1(\mathbf{v}) = - \sum_{\text{SP}} \left(\frac{(2\pi)^5}{\det \mathcal{A}_2} \right)^{1/2} E \sin(t'_{\text{SP}}) \times g_z(\mathbf{v} - \mathbf{A}(t'_{\text{SP}}), \mathbf{v}'_{\text{SP}} - \mathbf{A}(t'_{\text{SP}})) e^{-iS(\mathbf{v}, t_F, t'_{\text{SP}})} \times E \sin(t''_{\text{SP}}) d_z(\mathbf{v}'_{\text{SP}} - \mathbf{A}(t''_{\text{SP}})) e^{-iS(\mathbf{v}'_{\text{SP}}, t'_{\text{SP}}, t''_{\text{SP}})}, \quad (25)$$

where the saddle points are stationary points of the sum of actions $S(\mathbf{v}, t_F, t') + S(\mathbf{v}', t', t'')$, with respect to t' , t'' , and \mathbf{v}' . The second derivative matrix depends on t' , t'' , and \mathbf{v}' and, in particular, takes care of the quantum diffusion of the electronic wave packet within the time interval $[t'', t']$.

The saddle points are solutions of the following set of equations,

$$\frac{(\mathbf{v}'_{\text{SP}} - \mathbf{A}(t'_{\text{SP}} - \tau))^2}{2} + I_p = 0, \quad (26)$$

$$\frac{1}{\tau} \int_{t'_{\text{SP}} - \tau}^{t'_{\text{SP}}} \mathbf{A}(\tilde{t}) d\tilde{t} = \mathbf{v}'_{\text{SP}}, \quad (27)$$

$$\frac{(\mathbf{v} - \mathbf{A}(t'_{\text{SP}}))^2}{2} - \frac{(\mathbf{v}'_{\text{SP}} - \mathbf{A}(t'_{\text{SP}}))^2}{2} = 0, \quad (28)$$

where we have introduced the return time $\tau = t'_{\text{SP}} - t''_{\text{SP}}$.

The first of the above equations expresses the fact that in the limit $I_p \rightarrow 0$, the main contribution comes from the electrons that leave the nucleus at time t''_{SP} with zero kinetic momentum but with canonical momentum \mathbf{v}' . The second equation defines the value of \mathbf{v}' which allows the electron to return to the nucleus at t'_{SP} . Finally, the third

equation describes the rescattering process at t'_{SP} , and simply states that kinetic energy is conserved in rescattering. Note that neither the canonical nor the kinetic momenta have to be conserved at t'_{SP} . The kinetic momentum may undergo a change of sign, which we call backward scattering.

Generally, there are several pairwise complex conjugated families of solutions, to Eqs. (26–28). To obtain the desired solutions, one can use a method analogous to that developed in Ref. [10]. In the limit $I_p \rightarrow 0$, each of these families contains several values of τ corresponding to trajectories with single, double, etc., returns of the electron to the nucleus at t'_{SP} . Due to quantum diffusion, trajectories with a single return are the most relevant ones. The transverse spread of the trajectories reduces the number of strong rescattering events very rapidly. Returns after the first are most likely to have very large impact parameters. Even when we restrict ourselves to families of trajectories with single returns, there are still four kinds of families corresponding to different values of t'_{SP} . Each of the families contains an infinite number of solutions that shift $t'_{\text{SP}} \rightarrow t'_{\text{SP}} + 2\pi k$, where k is an integer. Only some of these families contribute to Eq. (25), however, since they must fulfill the condition that the imaginary parts of both $S(\mathbf{v}, t_F, t')$ and $S(\mathbf{v}', t', t'')$ be negative.

The analog of Eq. (24) becomes

$$b_1(\mathbf{v}) = - \sum_N \sum_{\text{SP}}' \left(\frac{(2\pi)^5}{\det \mathcal{A}_2} \right)^{1/2} \\ \times E \sin(t'_{\text{SP}}) g_z(\mathbf{v}, \mathbf{v}'_{\text{SP}}) e^{-iS(\mathbf{v}, t_F, t'_{\text{SP}})} \\ \times E \sin(t''_{\text{SP}}) d_z(\mathbf{v}'_{\text{SP}} - \mathbf{A}(t''_{\text{SP}})) e^{-iS(\mathbf{v}'_{\text{SP}}, t'_{\text{SP}}, t''_{\text{SP}})} \\ \times \delta(v^2/2 - N - I_p - U_p), \quad (29)$$

where \sum' restricts the sum to those saddle points for which $0 \leq \text{Im}(t'_{\text{SP}}) < 2\pi$. Again the above expression will display quantum interference.

For $\theta = 0$, $I_p = 0$, the saddle point equations become particularly simple. For instance, Eq. (28) implies that we deal either with forward scattering

$$v = v'_{\text{SP}}, \quad (30)$$

or backward scattering,

$$v = -v'_{\text{SP}} + 2A(t'_{\text{SP}}). \quad (31)$$

On the other hand, we have from Eq. (23)

$$t'_{\text{SP}} - \tau = \arccos(v'_{\text{SP}}/\sqrt{4U_p}), \quad (32)$$

i.e., $t'_{\text{SP}} - \tau$ is real provided v'_{SP} is real and $v'_{\text{SP}}/\sqrt{4U_p} \leq 1$.

One may ask how big v can be and still have real solutions of the saddle point equations, so that the probability amplitudes are nondecaying. For forward scattering the condition obviously is $v'_{\text{SP}}/\sqrt{4U_p} \leq 1$, i.e., $v^2/2 \leq 2U_p$. Therefore, in this limit, forward scattering is expected to affect only the low-energy part of the ATI spectrum. The case of backward scattering is a little trickier. Setting $2A(t'_{\text{SP}})$ to its extremal value $-\sqrt{4U_p}$, we find that $v \geq -3\sqrt{4U_p}$, giving $v^2/2 \leq 18U_p$. This

estimate turns out to be somewhat exaggerated, but it clearly indicates that backward scattering is more likely to contribute to the higher-energy part of the ATI spectrum. As we shall see below, that is indeed the case.

IV. MODEL ATOM

To calculate ATI spectra, we first have to specify the bare atomic matrix elements $\mathbf{d}(\mathbf{v})$ and $\mathbf{g}(\mathbf{v}, \mathbf{v}')$. In order to do this, we introduce a model atom with a separable short range potential. The results and conclusions obtained from this model should be applicable to systems with more realistic potentials since numerical calculations in Ref. [13] indicate that the appearance of rings and analogous structures in ATI spectra is a universal phenomenon which only weakly depends on the properties of the atom.

The stationary Schrödinger equation for the atom in the absence of the field, written in the momentum representation, is assumed to be

$$\frac{p^2}{2} \Psi(\mathbf{p}) - \frac{\gamma}{\sqrt{p^2 + \Gamma^2}} \int \frac{d^3 \mathbf{p}' \Psi(\mathbf{p}')}{\sqrt{(p')^2 + \Gamma^2}} = E \Psi(\mathbf{p}), \quad (33)$$

where γ and Γ are parameters related to I_p and the shape of the ground state wave function. Equation (33) supports one bound state corresponding to $E = -I_p$,

$$\Psi_0(\mathbf{p}) = \frac{\mathcal{N}}{(I_p + p^2/2)(p^2 + \Gamma^2)^{1/2}}, \quad (34)$$

where

$$\frac{4\pi^2 \gamma}{\Gamma + \sqrt{2I_p}} = 1, \quad (35)$$

and the normalization constant is

$$\mathcal{N}^2 = \frac{\sqrt{2I_p}(\Gamma + \sqrt{2I_p})^2}{4\pi^2}. \quad (36)$$

Similarly, the normalized scattering states corresponding to $E = p_0^2/2$ are given by

$$\Psi_{\mathbf{p}_0}(\mathbf{p}) = \delta(\mathbf{p} - \mathbf{p}_0) + \frac{B(\mathbf{p}_0)}{(p_0^2 - p^2/2 + i\epsilon)(p^2 + \Gamma^2)^{1/2}}, \quad (37)$$

where

$$B(\mathbf{p}_0) = -\frac{\gamma}{(p_0^2 + \Gamma^2)^{1/2}} \left(1 - \frac{4\pi i \gamma}{|p_0| + i\Gamma} \right)^{-1} \quad (38)$$

and ϵ is an infinitesimally small positive number.

Note that these states are appropriately normalized, i.e.,

$$\int d^3 \mathbf{p} \Psi_{\mathbf{p}_1}^*(\mathbf{p}) \Psi_{\mathbf{p}_2}(\mathbf{p}) = \delta(\mathbf{p}_1 - \mathbf{p}_2), \quad (39)$$

and correspond (depending on the sign of ϵ) to outgoing

or incoming boundary conditions.

After some elementary manipulations, we obtain

$$\mathbf{d}^*(\mathbf{p}_0) = -\frac{i\mathcal{N}\mathbf{p}_0[3p_0^2/2 + I_p + \Gamma^2]}{(p_0^2/2 + I_p)^2(p_0^2 + \Gamma^2)^{3/2}}, \quad (40)$$

and

$$\mathbf{g}(\mathbf{p}_1, \mathbf{p}_2) = \left\{ \begin{aligned} & \frac{-iB(\mathbf{p}_2)\mathbf{p}_1[3p_1^2/2 + I_p - p_2^2/2]}{(p_1^2 + \Gamma^2)^{3/2}} \\ & - \frac{iB^*(\mathbf{p}_1)\mathbf{p}_2[3p_2^2/2 + I_p - p_1^2/2]}{(p_2^2 + \Gamma^2)^{3/2}} \end{aligned} \right\} \\ \times \frac{1}{(p_2^2/2 - p_1^2/2 + i\epsilon)^2}. \quad (41)$$

Note that as expected $\mathbf{g}(\mathbf{p}_1, \mathbf{p}_2)$ is singular on the energy shell, i.e., when $p_1^2 = p_2^2$. This is an important feature since in the numerical calculations, we will have to regularize this singularity in a reasonable way.

V. RESULTS AND DISCUSSION

Our approach should be valid for $I_p/2U_p \leq 1$, i.e., in the regime where the interaction with the laser field is much more important to the evolution of the excited electron than its interaction with the ion core. However, in order to address the published xenon experiments [13] we will have to apply this model at the boundary, or even beyond the boundary of its validity. The saddle point method can still be employed to provide some insight into the ionization dynamics in this regime as long as the singularities in the atomic matrix elements are handled properly. Once more, we remind the reader that zeroth-order ionization amplitude is given by

$$b_0(\mathbf{v}) = i \int_0^{t_F} dt' E \sin(t') d_z(\mathbf{v} - \mathbf{A}(t')) e^{-iS(t_F, t', \mathbf{v})}, \quad (42)$$

which is easily evaluated numerically. It is much more difficult to evaluate the fivefold integral,

$$b_1(\mathbf{v}) = - \int_0^{t_F} dt' \int_0^{t'} dt'' \int d^3\mathbf{v}' E \sin(t') \\ \times g_z(\mathbf{v}, \mathbf{v}') e^{-iS(\mathbf{v}, t_F, t')} \\ \times E \sin(t'') d_z(\mathbf{v}' - \mathbf{A}(t'')) e^{-iS(\mathbf{v}', t', t'')}. \quad (43)$$

We note that if we actually carried out the integration over \mathbf{v}' , the singularity of $\mathbf{g}(\mathbf{v}, \mathbf{v}')$ would be effectively smoothed over as discussed in the preceding section. However, to keep the calculations manageable, we cannot explicitly perform this integration. We propose a simplified way out of this problem which reduces the fivefold integral into a twofold one. Namely, we perform the saddle point integration with respect to \mathbf{v}' , but leave the integrals over t' , and t'' as they stand. The saddle point is calculated with respect to quasiclassical actions only, so that

$$\mathbf{v}'_{\text{SP}}(t', \tau) = \frac{1}{\tau} \int_{t'-\tau}^{t'} \mathbf{A}(\tilde{t}) d\tilde{t}. \quad (44)$$

The result of saddle point integration for the fivefold integral (43) is obtained by setting

$$\mathbf{v}' = \mathbf{v}'_{\text{SP}}(t', \tau), \quad (45)$$

and substituting

$$\int d^3\mathbf{v}' \rightarrow \left(\frac{\pi}{\epsilon + i\tau/2} \right)^{3/2} \quad (46)$$

for the integration over \mathbf{v}' . The latter factor accounts for quantum diffusion effects. The remaining twofold integration over t' and τ in Eq. (43) can be performed numerically relatively easily.

Unfortunately, since we calculate the saddle points using the stationarity condition for the quasiclassical action, the resulting integrals still contain a singularity of the form

$$\frac{1}{[(\mathbf{v} - \mathbf{A}(t'))^2/2 - (\mathbf{v}'_{\text{SP}}(t', \tau) - \mathbf{A}(t'))^2/2 + i\epsilon]^2}. \quad (47)$$

For purposes of efficient numerical simulation we smooth this singularity, allowing ϵ to be of the order of 1. As stated above, such smoothing takes place when more exact methods of evaluation of the integral over \mathbf{v}' are used. For instance, if we include corrections to the saddle point coming from the \mathbf{v}' dependence of $d_z(\mathbf{v}' - \mathbf{A}(t' - \tau))$, $\mathbf{v}'_{\text{SP}}(t', \tau)$ becomes complex and the singularity (47) is no longer encountered for real t' and τ (compare a discussion of the so called Gaussian model in Ref. [10]). This is effectively equivalent to choosing a finite value for ϵ . We should stress, however, that although our results depend on the value of ϵ , the dependence is relatively weak, affecting mainly the magnitude but not the shape of those parts of the spectrum that come from rescattering events.

We first consider the angular distributions obtained from direct numerical integration of the TDSE corresponding to the case studied in Ref. [13]: xenon at a wavelength of 1064 nm and intensities in the range 10–30 TW/cm². These calculations, which show pronounced rings on the ATI peaks with energies near $8U_p$, are known to be in good agreement with the experimental results. It is most illustrative to consider the emission into a narrow cone as a function of the scattering angle, θ , measured from the laser polarization direction. In this way, we can describe the behavior of the energy distributions, observing how they change, in particular, how the observed structure evolves as the direction of emission is changed. We show representative results for two intensities 2 and 3×10^{13} W/cm² in Fig. 1 for $\theta = 0^\circ, 20^\circ, \text{ and } 40^\circ$. In all figures, the distributions are plotted in terms of the electron energy scaled by the ponderomotive energy. In both cases shown, the emission, as expected, is generally strongest along the polarization axis. Also, both on-axis distributions show a very pronounced dip between $8U_p$ and $9U_p$, followed by a plateau and a cutoff above $11U_p$. As θ increases, the dip, plateau and cutoff move to lower energies, so that for some off-axis angle the maximum will

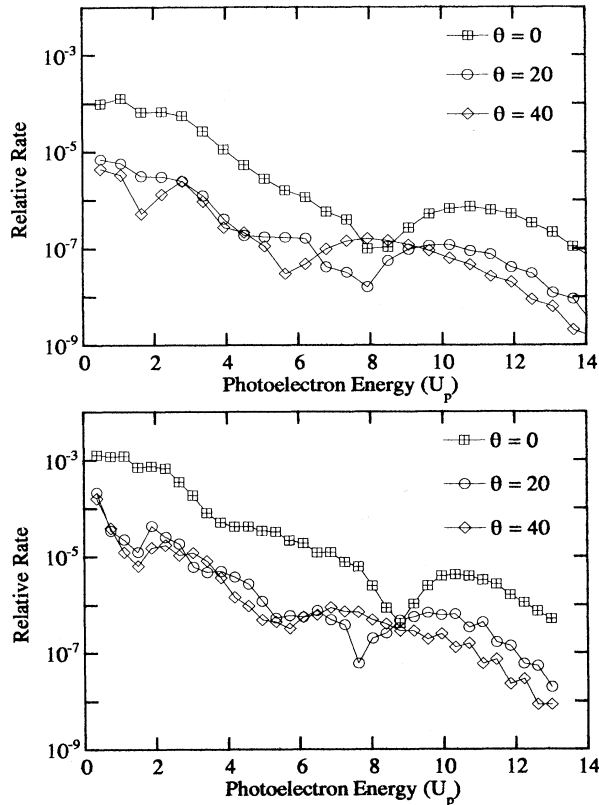


FIG. 1. Calculated fixed-angle photoelectron spectra for xenon at $\lambda = 1.064 \mu\text{m}$ and intensities of 2 (upper plot) and 3 (lower plot) $\times 10^{13} \text{ W/cm}^2$ from the numerical integration of the single-active-electron time-dependent Schrödinger equation. θ is the scattering angle (in deg) measured from the direction of polarization of the laser.

appear at the same energy as the on-axis dip. This produces the observed ring structure. Recent experiments by Paulus *et al.* [29] which measured the photoelectron spectrum in a narrow region around the polarization axis showed the pronounced dip and plateau found in these calculations. The distributions are generally narrower at low energies and become broader at the high-energy end. As discussed above, the two-step model predicts that the high-energy ATI peaks can only come from a rescattering process, so that one might expect their angular distributions to be broader [2]. It is these general characteristics of the spectrum we wish to interpret in terms of our semiclassical calculations.

Since our semiclassical analysis is based on specific trajectories we can easily investigate the dynamics of rescattering, distinguishing between scattering which does not alter the kinetic momentum of the electron appreciably, forward scattering, and those contributions to the spectrum which come from backward scattering events in which the sign of the kinetic momentum reverses. We can trivially separate the direct tunneling spectra one would observe in the absence of rescattering by considering only the contribution from the lowest order term in our expansion given by Eq. (42). Solutions to Eq. (43)

provide the redistribution of electron canonical momenta due to the rescattering events.

In these calculations, we have considered combinations of parameters to give a picture of the dependence of the ATI angular structures on the laser wavelength and intensity. We present results for four cases, shown in Figs. 2–5, that all exhibit off-axis emission, rings or broadening, for some small energy range within the higher-energy ATI peaks. In the first three cases presented, we use the parameters within the expected range of validity of the GSFA, i.e., for $I_p/2U_p \leq 1$. In Fig. 5, we plot the results for parameters corresponding approximately to experiment of Ref. [13], i.e., $I_p = 10$, and $U_p = 3$, where we continue to express these quantities in units of the photon energy. We will refer to this as the 10-3 case, and similarly for the others.

Figures 2–5 each consist of four plots. The upper left-hand plot shows the total emission into a given angle, for $\theta = 0^\circ$, 20° , and 40° , including the direct tunneling component and that from the first-order rescattering term: $|b_{\text{full}}(\mathbf{v})|^2 = |b_0(\mathbf{v}) + b_1(\mathbf{v})|^2$. These can be compared directly to the numerical results shown in Fig. 1. In the other three plots, we break down the separate contributions for the three angles considered. In addition to the total (full) yield, we show the spectra (i) for direct tunneling only, $|b_{\text{Tunn}}(\mathbf{v})|^2 = |b_0(\mathbf{v})|^2$; (ii) taking into account rescattering into the forward hemisphere only, $|b_F(\mathbf{v})|^2 = |b_1^+(\mathbf{v})|^2$, where we use the same expression for $b_1^+(\mathbf{v})$ as in the full first-order term except that we include only those values of $\mathbf{v}'_{\text{SP}}(t', \tau)$ for which $\mathbf{v} \cdot \mathbf{v}'_{\text{SP}} \geq 0$; and (iii) for the backward rescattering component, $|b_B(\mathbf{v})|^2$, which is restricted to velocities such that $\mathbf{v} \cdot \mathbf{v}'_{\text{SP}} < 0$.

In Figs. 2–4, we show the results for the tunneling cases we have considered. In Fig. 2, the 3-3 case results are presented. This case represents short wavelength and moderately strong intensity. An example might be a doubled dye laser ionization of xenon at about 10^{14} W/cm^2 . The high intensity complement to this case is the 3-10 case shown in Fig. 3, which corresponds to the previous example with an intensity 3.3 times higher. The last tunneling case we have studied is 10-10, long wavelength but high enough intensity to reach the tunneling regime. This case would be representative of exciting xenon at approximately $1 \mu\text{m}$ at an intensity of just over 10^{14} W/cm^2 or helium with doubled Nd:YAG at about 10^{15} W/cm^2 . The ionization rates for all these cases would be very high, requiring subpicosecond pulses to probe the regime.

In the results shown in these three Figs. (2–4), we can see some general trends in the angle-dependent yields (the upper left-hand plot in each figure). We note first, that the results below $(2-3)U_p$ are found not to be very reliable. The first-order theory is probably inadequate for these low-energy electrons. In all cases, there is a pronounced angular dependent cutoff in the yield: approximately at $11U_p$ on axis, decreasing to $(7-8)U_p$ at $\theta = 40^\circ$. Initially the yields fall with increasing energy, not always monotonically, approximately following the tunneling rates (see the open circles in the other three plots in each figure), then show an abrupt change of slope, or a dip in the spectrum. This break in slope is angle dependent.

dent, decreasing with increasing angle because of the very narrow angular dependence of the direct tunneling component. Obviously, all the electrons with energies higher than the tunneling component must have been created through rescattering. On axis, the change of slope occurs near $8U_p$ for the 3-3 case and shifts to around $6U_p$ for the 3-10 and 10-10 cases. In the latter two cases, we also find a peak in the spectrum at the cutoff. This seems to be a classical rainbow effect which is washed out if we increase the value of the parameter ϵ in Eq. (47). The peak becomes sharper if ϵ is reduced. The dips apparently are due to interference between tunneling electrons which have not rescattered and rescattered electrons at the same energy. The dips appear in the total spectrum at the point where the yields from these two components are of comparable magnitude. When the tunneling rate drops more quickly with energy, as in the 10-10 case, for example, the break in slope, or dip will appear at a lower energy. We see evidence of rings, but those in the calculations for 3-10 and 10-10 may be artifacts of the sharp peak at the cutoff. In any case, we consistently find that the rescattering electrons have much broader angular dis-

tributions than the direct tunneling component, becoming approximately flat in the two cases just mentioned. Finally, one very important point which comes from this analysis is that the high-energy photoelectrons in these three cases where our ansatz is valid are produced exclusively by backscattering.

Our results, shown in Fig. 5, for the case which approximates the published xenon data and the calculations represented in Fig. 1 are not in the tunneling regime, $I_p/2U_p > 1$. In spite of this the angular yields display a similarity to the "exact" results. The yields still extend to approximately $11U_p$ on axis, have a noticeable dip near $9U_p$, and will exhibit a ring at this energy roughly 20° off axis. Also, the zeroth-order distribution, which we can no longer legitimately call the tunneling component, is found to be very narrow and drops off very quickly with energy. As in the previous cases, the high-energy electrons are produced by backscattering only. However, there are some significant differences between these results and those from the three cases just described. First, the first-order, or rescattering, term turns out to be much larger than the zeroth-order term.

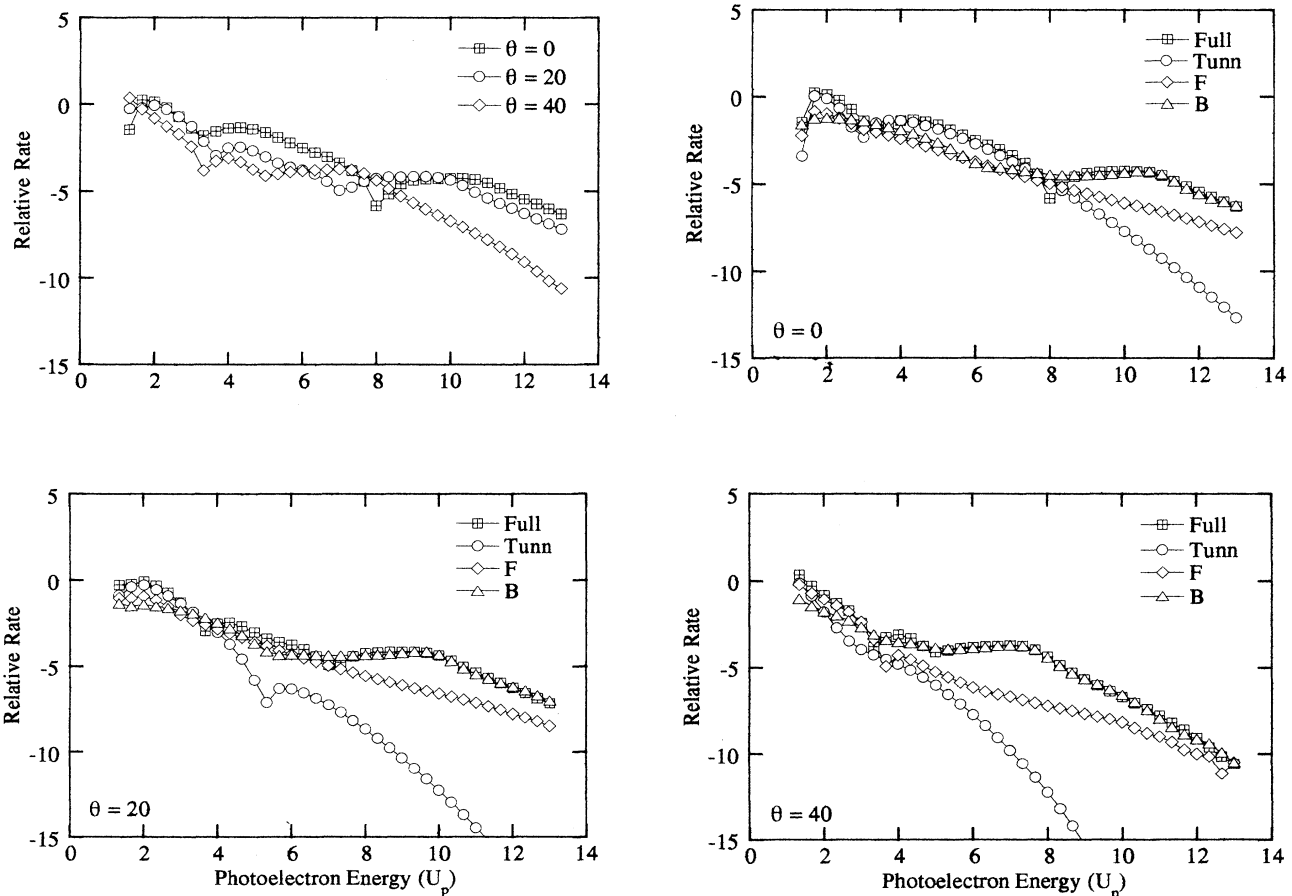
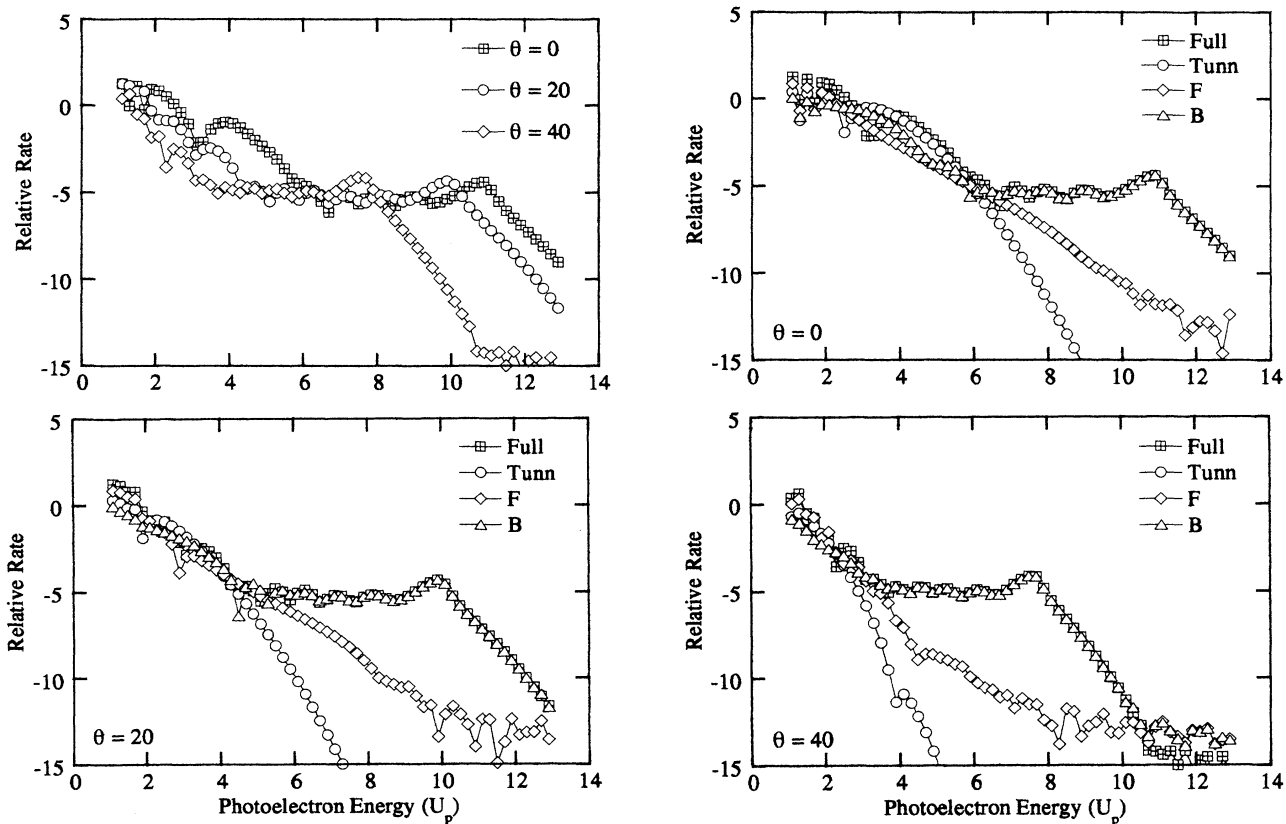
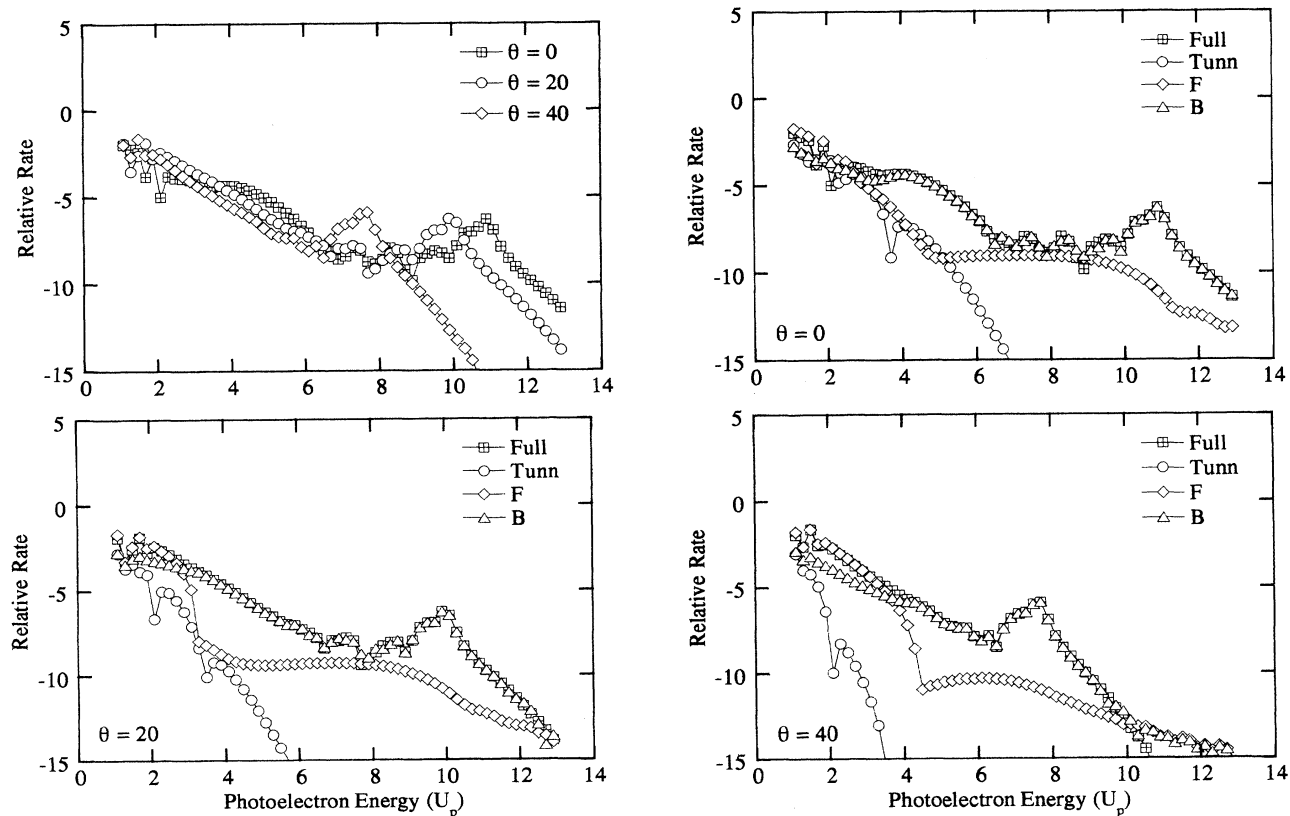


FIG. 2. Quasi-classical fixed-angle photoelectron spectra for the case $I_p = 3$ and $U_p = 3$. Plotted are \log_{10} (relative rates). Upper left plot shows the total (full) spectra including the zeroth- and first-order terms. The other three plots show the separate contributions to the full spectra. Tunn is the direct tunneling component (the zeroth-order term), F and B designate the first-order terms corresponding to rescattering into the forward and backward directions, respectively.

FIG. 3. Same as Fig. 2, but for $I_p = 3$ and $U_p = 10$.FIG. 4. Same as Fig. 2, but for $I_p = 10$ and $U_p = 10$.

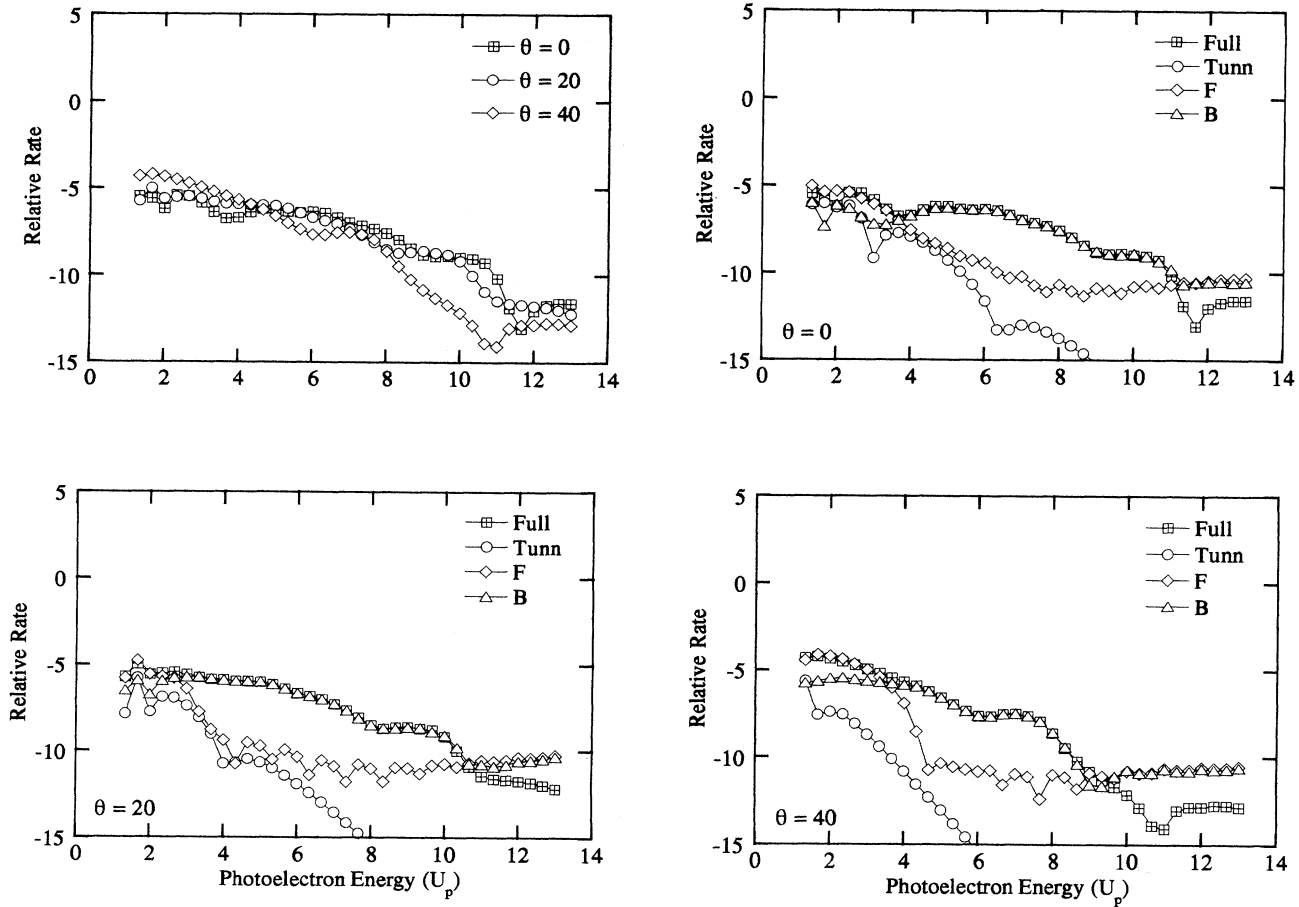


FIG. 5. Same as Fig. 2, but for $I_p = 10$ and $U_p = 3$. This approximates the case shown in the lower plot of Fig. 1.

This indicates that our perturbation expansion in terms of the atomic potential actually breaks down, or at best converges more slowly. Many electron trajectories will stay close to the ion core, probably experiencing many interactions with the core. It is not feasible to calculate higher-order terms in the perturbation expansion with the technique we have used here, as the number of contributing trajectories quickly gets out of hand. However, there are reasons to believe that this proliferation of relevant trajectories concerns only the slow electrons. Once an electron gains more than $(2-3)U_p$ in energy in the first rescattering act, it is not likely that it will not return to the ion core. The perturbation series should, thus, converge more quickly for the higher-energy electrons. Clearly, the size of the rescattering term indicates that in the low intensity regime, an electron is much more likely to have significant interactions with the ion core after being excited into the continuum. Second, the on-axis dip in Fig. 5 is not due to interference between the zeroth-order and first-order terms, as in the cases above, but appears in the rescattering term alone. We find the existence of this dip does not depend on the only adjustable parameter in our theory, ϵ , but the strength of the first-order spectrum does, scaling approximately as

ϵ^{-2} . The origin of the scattering ring, in this case, is not clear from these calculations.

In all four cases studied, we found a sharp decrease in the yields at particular scaled energies which depended on the scattering angle. A simple analysis of our stationary phase conditions shows where the cutoff should appear. Given the conditions in Eqs. (26)–(28), and considering the case $I_p = 0$, we can calculate the largest real velocity that satisfies these equations. If we evaluate the corresponding energy as a function of the time between emission and rescattering, τ , we obtain the angle dependent cutoff energies for the spectra. These predicted maxima are shown in Fig. 6. Here, $\theta = 0$ is forward and $\theta = \pi$ is backward scattering. The maximum is $10U_p$ for a scattering angle of π and for one particular value of τ . It decreases with changes in either the propagation time or scattering angle. The agreement between these predictions and the beginning of the high-energy decline in each spectrum shown in Fig. 1 indicates the classical analysis of the electron dynamics within the continuum, ignoring the perturbations of the ion core potential, is valid for predicting the limits of the energy distributions.

In conclusion, we have investigated photoelectron dynamics using a quasiclassical formalism based on a per-

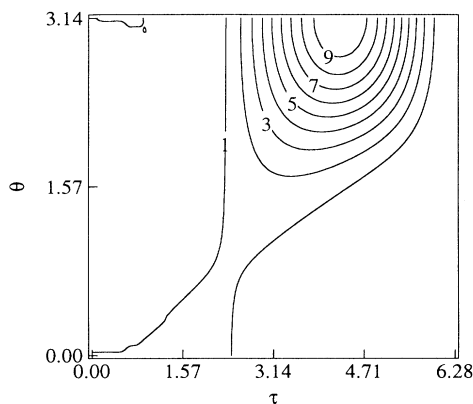


FIG. 6. Contour plot of the maximum rescattering energy as a function of the propagation time between emission and scattering, τ , and scattering angle θ (in rad) (in units of $1/\omega$).

turbation expansion in the atomic potential. The initiation step is calculated numerically, providing the spectrum of electron energy and angular distributions produced by the transition into the continuum. The electron motion within the continuum between scattering events is given by the classical equations of motion for a free electron in the laser field. The first-order term in our perturbative expansion gives the effect on the electron trajectories of a single collision with the parent ion core. The scattering integral is evaluated using a station-

ary phase approximation. The predicted electron spectra in the tunneling regime show a high energy broad component which is due to backward scattering of the electrons. In the parameter regime relevant to recent experiments on xenon at $1\ \mu\text{m}$, the spectrum from the rescattering term is in qualitative agreement with the measurements and with numerical solutions to the time-dependent Schrödinger equation. The spectra show rings for electron energies near $(8-9)U_p$. These first-order results resemble those obtained by Becker *et al.* [30] using a very similar model. Our analysis shows that all high-energy electrons in this spectrum are produced by backward scattering of the returning electrons. At this point we can only say that in the low intensity regime, we obtain results which qualitatively agree with the recent experiments in xenon. We hope that measurements will become available in the tunneling regime, where our prediction of flatter angular distributions beginning well below the $8U_p$ is expected to be more reliable.

ACKNOWLEDGMENTS

This paper grew out of a workshop at the NSF Center for Ultrafast Optical Science at the University of Michigan. This work was carried out in part under the auspices of the U.S. DOE under Contract No. W-7405-ENG-48. M.L. and K.C.K. wish to thank the staff of the JILA Visiting Fellowship Program for their hospitality and financial support.

-
- [1] H. G. Muller, *Comm. At. Mol. Phys.* **24**, 355 (1990). See also, W. Becker, R. R. Schlicher, and M. O. Scully, *J. Phys. B* **19**, L785 (1986).
- [2] K. C. Kulander, K. J. Schafer, and J. L. Krause, in *Super-Intense Laser-Atom Physics*, Vol. 316 of *NATO Advanced Study Institute, Series B: Physics*, edited by B. Piraux, A. L'Huillier, and K. Rzażewski (Plenum Press, New York, 1993).
- [3] P. B. Corkum, *Phys. Rev. Lett.* **71**, 1994 (1993).
- [4] A. L'Huillier and Ph. Balcou, *Phys. Rev. Lett.* **70**, 774 (1993).
- [5] J. J. Macklin, J. D. Kmetec, and C. L. Gordon III, *Phys. Rev. Lett.* **70**, 766 (1993).
- [6] J. L. Krause, K. J. Schafer, and K. C. Kulander, *Phys. Rev. Lett.* **68**, 3535 (1992).
- [7] L. V. Keldysh, *Zh. Eksp. Teor. Fiz.* **47**, 1945 (1964) [*Sov. Phys. JETP* **20**, 1307 (1965)]; F. Faisal, *J. Phys. B* **6**, L312 (1973); H. R. Reiss, *Phys. Rev. A* **22**, 1786 (1980).
- [8] M. V. Ammosov, N. B. Delone, and V. P. Kraĭnov, *Zh. Eksp. Teor. Fiz.* **91**, 2008 (1986) [*Sov. Phys. JETP* **64**, 1191 (1986)]; N. B. Delone and V. P. Kraĭnov, *J. Opt. Soc. Am. B* **8**, 1207 (1991); V. P. Kraĭnov and V. M. Ristić, *Zh. Eksp. Teor. Fiz.* **101**, 1479 (1992) [*Sov. Phys. JETP* **74**, 789 (1992)].
- [9] A. L'Huillier, M. Lewenstein, P. Salières, Ph. Balcou, M. Yu. Ivanov, J. Larsson, and C. G. Wahlström, *Phys. Rev. A* **48**, 3433 (1993).
- [10] M. Lewenstein, Ph. Balcou, M. Yu Ivanov, Anne L'Huillier, and P. Corkum, *Phys. Rev. A* **49**, 2117 (1994).
- [11] R. P. Feynmann and A. R. Hibbs, *Quantum Mechanics and Path Integrals* (McGraw-Hill, New York, 1965).
- [12] B. Yang, K. J. Schafer, B. Walker, K. C. Kulander, P. Agostini, and L. F. DiMauro, in *Proceedings of the International Conference on Multiphoton Processes VI*, edited by D. K. Evans (World Scientific, Singapore, 1993).
- [13] B. Yang, K. J. Schafer, B. Walker, K. C. Kulander, P. Agostini, and L. F. DiMauro, *Phys. Rev. Lett.* **71**, 3770 (1993).
- [14] D. Feldman, *Proceedings of the International Conference on Multiphoton Processes VI*, edited by D. K. Evans (World Scientific, Singapore, 1993).
- [15] K. C. Kulander and K. J. Schafer, *Proceedings of the International Conference on Multiphoton Processes VI*, edited by D. K. Evans (World Scientific, Singapore, 1993).
- [16] K. J. Schafer and K. C. Kulander, *Proceedings of the International Conference on Multiphoton Processes VI*, edited D. K. Evans (World Scientific, Singapore, 1993).
- [17] M. Lewenstein, J. Mostowski, and M. Trippenbach, *J. Phys. B* **18**, L461 (1985); J. Grochmalicki, J. R. Kukliński and M. Lewenstein, *ibid.* **19**, 3649 (1986).
- [18] Th. Auguste, P. Monot, L. A. Lompré, G. Mainfray, and

- C. Manus, *J. Phys. B* **25**, 4181 (1992).
- [19] E. Mevel, P. Breger, R. Trainham, G. Petite, P. Agostini, A. Migus, J.-P. Chambaret, and A. Antonetti, *Phys. Rev. Lett.* **70**, 406 (1993).
- [20] M. H. Mittleman, *Theory of Laser-Atom Interactions*, 2nd ed. (Plenum Press, New York, 1993).
- [21] See, for instance, the contribution of H. R. Reiss, in *Super-Intense Laser-Atom Physics*, Vol. 316 of *NATO Advanced Study Institute, Series B: Physics*, edited by B. Piraux, A. L'Huillier, and K. Rzażewski, (Plenum Press, New York, 1993).
- [22] Even that simplification can be avoided and we can account for the influence of the bound states, as discussed in Ref. [17], and in M. Lewenstein and L. Plaja (unpublished).
- [23] N. M. Kroll and K. M. Watson, *Phys. Rev. A* **8**, 804 (1973).
- [24] F. V. Bunkin and M. V. Fedorov, *Zh. Eksp. Teor. Fiz.* **49**, 1215 (1965) [*Sov. Phys. JETP* **22**, 844 (1966)].
- [25] S. Bivona, R. Burlon, R. Zangara, and G. Ferrante, *J. Phys. B* **18**, 3149 (1985).
- [26] A. Weingartshofer, E. M. Clarke, J. K. Holmes, and C. Jung, *Phys. Rev. A* **19**, 2371 (1979).
- [27] M. Lewenstein and Ph. Balcou (unpublished).
- [28] Ph. Bucksbaum (unpublished), B. Yang, K. J. Schafer, B. Walkerm, K. C. Kulander, L. F. DiMauro, and P. Agostini, in *Quantum Optics III*, Proceedings of the International Conference, Szczyrk 1993, Poland, edited by M. Kolwas and J. Mostowski, special issue of *Acta Phys. Pol.* **86**, 41 (1994).
- [29] G. G. Paulus, W. Nicklich, H. Xu, P. Lambropoulos, and H. Walther, *Phys. Rev. Lett.* **72**, 2851 (1994).
- [30] W. Becker, A. Lohr, and M. Kleber (unpublished).